Eur. Phys. J. B **43**, 163–174 (2005)
DOI: 10.1140/epjb/e2005-00039-1

THE EUROPEAN PHYSICAL JOURNAL B

Uncompensated antiferromagnetic structure of Ho_2Ni_2Pb

K. Prokeš[1,a], E. Muñoz Sandoval[2], A.D. Chinchure[3], and J.A. Mydosh[4]

[1] Hahn-Meitner-Institute, SF-2, Glienicker Str. 100, 141 09 Berlin, Germany
[2] Advanced Materials Department, IPICyT, Apartado Postal 3-74,Tangamanga, 78231 San Luis Potosi, SLP, Mexico
[3] Materials Research Laboratory, John F. Welch Technology Center, Bangalore - 560 066, India
[4] Kamerlingh Onnes Laboratory, Leiden University, 2300 RA Leiden, The Netherlands and Max-Planck-Institute for Chemical Physics of Solids, 01187 Dresden, Germany

Received 6 July 2004 / Received in final form 6 December 2004
Published online 25 February 2005 –

Abstract. We have studied the magnetic structure of the orthorhombic compound Ho_2Ni_2Pb by means of neutron diffraction in zero field and in magnetic fields up to 4.5 T. Both powder and single-crystalline samples were used. Previous bulk measurements suggest two distinct magnetic phase transitions: one at $T_N = 7.0$ K and the other at 4.8 K. Our neutron diffraction measurements, which were made in the range 1.5−20 K, showed that Ho_2Ni_2Pb has a collinear magnetic structure with unequal number of up and down Ho moments that are aligned parallel and antiparallel to the c axis. At the lowest temperatures the Ho moments are equal in size, each 8.3 μ_B in agreement with magnetization data. The magnetic structure can be described as having a $5a \times b \times c$ magnetic unit cell. Below $T_s = 3.0$ K the structure is squared up. A smooth development of all the magnetic moment magnitudes indicates that the magnetic structure remains in principle the same over the whole temperature range, the "phase transition" around 4.8 K can be identified as an inflection point in the temperature dependence of one of the Ho moments. With increasing temperature there is a clear development towards a simple transverse sine-wave modulated magnetic structure that is established just below T_N.

PACS. 75.50.-y Studies of specific magnetic materials – 75.25.+z Spin arrangements in magnetically ordered materials (including neutron and spin-polarized electron studies, synchrotron-source X-ray scattering, etc.) – 75.50.Ee Antiferromagnetics

1 Introduction

Novel magnetic compounds are currently the subject of intensive fundamental and applied research [1]. Recently, several new rare-earth (R) intermetallic compounds with the stoichiometry 2:2:1 were synthesised [2]. Rare-earth elements from Gd to Lu and Y can be combined with Ni and Pb. Detailed bulk measurements suggest that the only magnetic element in these materials is the rare-earth ion [3,4]. The last two elements do not carry any magnetic moment. The crystal structure has orthorhombic symmetry of the Mn_2AlB_2 type and the space group $Cmmm$ [2]. This structure type is also denoted as the AlB_2Fe_2 in the literature [5]. All the R atoms are equivalent – they occupy the same crystallographic position 4(j). Due to the surroundings of the R atoms with non-magnetic elements, there exists, however, a significant magnetocrystalline anisotropy. Multiple magnetic phase transitions observed in these compounds [4,6] suggest that complex magnetic moment arrangements can be expected as a result of competing magnetic interactions.

On the basis of bulk measurements on polycrystalline [3,7,8] and single crystalline [4] Ho_2Ni_2Pb samples it was suggested that two different magnetic phases exist at low temperatures in this system. Concerted magnetic susceptibility, magnetization, specific heat and electrical resistivity measurements indicated that Ho_2Ni_2Pb orders antiferromagnetically at $T_N = 7.0$ K, the other magnetic phase transition at $T_m = 4.8$ K is considered as being antiferromagnetic to ferromagnetic in nature [4,7,8]. In contrast, Gulay et al. [3] report for Ho_2Ni_2Pb ferromagnetic phase transition taking place at $T_C = 7.0$ K. According to them, no other magnetic phase transition appears in this system down to 4.2 K. Thus, one encounters a rather rare case when two groups report for a magnetic substance having large magnetic moments entirely different ground states although they agree upon the value of the magnetic phase transition temperature.

Magnetization measurements on single-crystalline samples suggest that low-temperature phases are very

[a] e-mail: prokes@hmi.de

sensitive in an anisotropic way to applied magnetic fields. This is reflected in sharp metamagnetic transitions and a giant magnetoresistance accompanying these transitions [4]. The strongest magnetic response had been found for the a axis and the weakest for the b axis, which was qualified as the hard magnetization direction. The saturated magnetization reaches about 8 μ_B/Ho [4].

Similar magnetic properties as in Ho_2Ni_2Pb were detected for Dy_2Ni_2Pb [4]. Later, however, combined experiments on Dy_2Ni_2Pb [9] showed that although bulk measurements suggested two magnetic phase transitions, neutron diffraction measurements revealed existence of one single antiferromagnetic (AF) phase having two temperature-dependent propagation components.

In order to clarify the connection between the rather complicated bulk magnetic behavior of Ho_2Ni_2Pb and its microscopic magnetic structure, we have investigated this material by means of neutron diffraction at low temperatures. As doubts regarding the type of the magnetic phase transitions at ≈7.0 K and ≈4.8 K as determined from bulk measurements exist, our main aim is to reveal the magnetic structures at low temperatures which might include multiple propagation vectors. This should give us unambiguous information as to what kind of magnetic phase transitions are taking place in this system. Application of a magnetic field on a powder sample containing free-to-rotate grains was used to identify the easy magnetization direction in this material.

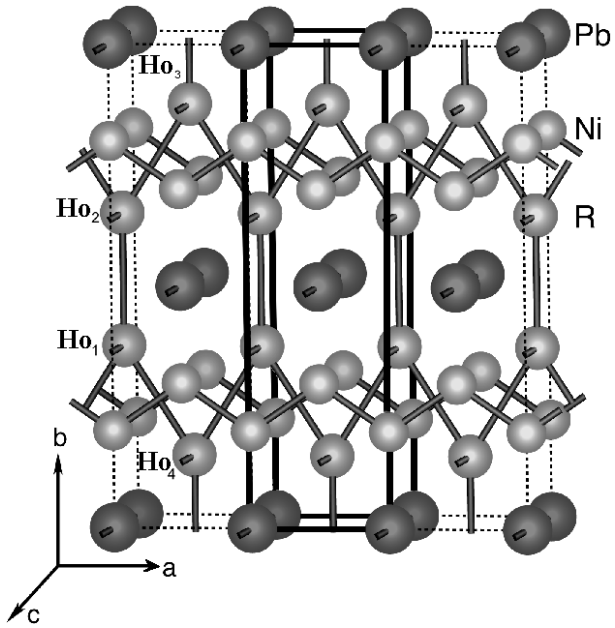

Fig. 1. Orthorhombic crystal structure (*Cmmm*) of R_2Ni_2Pb (R stands for Gd to Lu and Y). The unit cell is indicated by the dark lines. The largest, medium, and the smallest spheres represent Pb, R, and Ni atoms, respectively. The labeling Ho_1, Ho_2, Ho_3 and Ho_4 is used below in an a-c projection to designate the magnetic structure.

2 Experimental

Ho_2Ni_2Pb compound possess a highly anisotropic crystal structure (Fig. 1). It has the orthorhombic symmetry (space group *Cmmm* - number 65) [5] with the b axis more than four times longer than the other two principal axes. As a consequence, there is a significant difference in the growth rate, being much higher along the b axis. The result is a natural multilayer structure that consists of $a-c$ planes of various kinds stacked along the b axis direction. R atom planes are intercalated between Pb and Ni planes in the sequence: Pb - R - Ni - R - Pb - R - Ni - R - Pb. All the R atoms in the unit cell occupy the 4(j) position and are thus crystallographically equivalent. The sample were prepared by arc melting pure elements under purified Ar atmosphere. After flipping and remelting the ingots a few times in order to achieve good homogeneity the sample was heat-treated for 72 hours at 870 K. Finally, determination of the stoichiometry and homogeneity using electron probe micro-analysis (EPMA) was conducted. The samples have been found to contain about 5 vol.% of a secondary phase, probably HoNiPb. Within 2% resolution, the main phase has been found to have the desired 2:2:1 stoichiometry.

Several small single crystals with dimensions of about $1.5 \times 1.5 \times 0.3$ mm^3 have been extracted from a highly textured polycrystalline material. The Laue X-ray method and EPMA were used to control their quality. The best quality single crystal has been then used in the neutron-diffraction experiment.

Neutron-diffraction patterns were collected at 1.5, 5 and 20 K using the multicounter diffractometer E6 installed at the Berliner Neutron Scattering Center BENSC at the Hahn-Meitner-Institute. A standard ILL orange cryostat has been employed to achieve low temperatures. We have also collected at low temperatures a few powder diffraction patterns on the double axis diffractometer E4 in magnetic fields up to 4.5 T generated by a superconducting magnet. Finally, we have also studied on E4 the small single crystal in zero field and in the temperature range between 1.6 and 20 K. The incident neutron wave length was 2.44 Å in all cases. For the powder measurements about 7 g of Ho_2Ni_2Pb was ground under inert atmosphere and encapsulated in a vanadium container with He gas. The data were collected in the case of E6 measurements for about 12 hours (3 hours at each of the four detector positions, each covering 20 degrees) at each temperature and analyzed by means of the Rietveld profile procedure [10] using the program Fullprof [11]. The Ho magnetic form factor was taken from Sears et al. [12]. In the case of the E4 measurements we collected each powder pattern typically during four hours. Here, however, the detector was moved in a step-by-step manner to cover the whole range leading to lower counting rates. To trace magnetic phase transitions we have also followed the temperature development of peak intensities by measuring a 40 degrees wide diffraction range at 70 different temperatures for about 20 minutes each. Similar temperature dependence study was also done using the single crystal.

3 Results

3.1 Paramagnetic state

Inspection of the powder neutron diffraction pattern recorded at 20 K, in the paramagnetic state of Ho_2Ni_2Pb, revealed that it is impossible to index all the observed reflections (although all the reflections not indexed were of very small intensity) within the space group *Cmmm* reported for this compound in literature [2]. Since we knew that about 5 vol.% of most probably HoNiPb is present in our sample we have tried to include this compound in the refinement. HoNiPb is reported to form in the orthorhombic TiNiSi type of structure (space group *Pnma* - no. 62) [13]. Indeed, after including HoNiPb into the refinement we were able to index all the observed peaks. The quality of the fit was improved by more than a factor of two. According to the best fit 4.9 vol.% of HoNiPb is present in the sample, in excellent agreement with EPMA results.

Systematic extinction rules for the main phase Ho_2Ni_2Pb are in agreement with the reported space group *Cmmm* for this system. Full Rietveld-type refinement that included two sets of phase-dependent parameters, one for Ho_2Ni_2Pb and the other for HoNiPb (such as scale factors, lattice cell parameters, positional parameters and isotropic overall temperature Debye-Waller factors of atoms) together with extrinsic parameters (such as background) confirm the orthorhombic Mn_2AlB_2 type of structure for the Ho_2Ni_2Pb phase and the TiNiSi type for the secondary HoNiPb phase.

In the case of Ho_2Ni_2Pb there are four Ho atoms in the crystallographic unit cell and all the Ho atoms occupy the 4(j) 0 y 0.5 Wyckoff position with local symmetry m 2 m. For the sake of discussion made below we label these atoms as Ho_1 (at 0 y_{Ho} 0.5), Ho_2 (at 0 $-y_{Ho}$ 0.5), Ho_3 (at 0.5 0.5+y_{Ho} 0.5) and Ho_4 (at 0.5 0.5$-y_{Ho}$ 0.5). Ni atoms, which are in this material non-magnetic [4,14] occupy the 4(i) 0 y 0 position and Pb the 2(a) 0 0 0 position. There are four Ni and two Pb atoms in the crystallographic unit cell.

In the case of HoNiPb there are four atoms of each kind in the unit cell, all of them occupying the 4(c) position, however, with different positional parameters.

Results of the best fit (shown in Fig. 2) to diffraction data at 20 K are summarized in Table 1. Inclusion of the occupation parameters to the fit as free parameters did improve further on the quality of the fit. Deficiency of Ni and Pb of the order of 2–3 at.% has been detected. The actual stoichiometry of the main phase in our sample is $Ho_2Ni_{1.96}Pb_{0.97}$, close to the desired 2:2:1 ratio and in agreement with EPMA result. Due to the highly anisotropic shape of the crystallographic unit cell we had to include also a preferential orientation parameter in order to account for a preferential orientation of the needle-like crystallites. The low intensity of reflections belonging to HoNiPb did not allowed us to determine all the structural details for this phase with sufficient quality. The refined lattice parameters of HoNiPb at 20 K are: a = 705.5(1.0) pm, b = 447.4(0.4) pm and c = 769.6(1.2) pm.

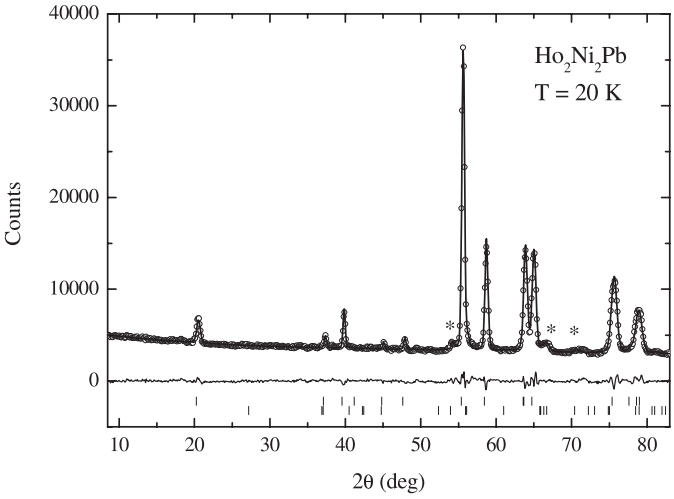

Fig. 2. The diffraction data (circles) of Ho_2Ni_2Pb taken in the paramagnetic state at 20 K together with the best fit (the full line through points) and the difference between them (line at the bottom). Crystal structure Bragg reflection positions belonging to the main Ho_2Ni_2Pb phase and to HoNiPb impurity phase are tick-marked at the bottom (for HoNiPb being the lower). By stars we denote three of the strongest HoNiPb reflections). For numerical results see Table 1.

Table 1. Refined structural parameters of Ho_2Ni_2Pb determined above the upper magnetic phase transition in the paramagnetic state at 20 K.

Space group:	*Cmmm*	T = 20 K
Atom,site	Pos. parameters	Occupation
Ho, 4(j)	0 0.3649(4) 0.5	1.00 (fixed)
Ni, 4(i)	0 0.1990(5) 0	0.98 (1)
Pb, 2(a)	0 0 0	0.96 (1)
Lattice constants:		
a = 400.34(9) pm	b = 1391.7(3) pm	c = 361.5(1) pm
Agreement factors:		
χ^2 = 5.26	R_p = 2.66%	R_B = 2.35%

3.2 Identification of propagation vectors

As the temperature is lowered below the putative magnetic phase transition temperature of 7.0 K, new Bragg reflections in the diffraction pattern appear. These reflections are considered to be due to magnetic order. In Figure 3 we show the contour intensity plot resulting from 70 low-angle scans. As can be seen, the phase transition determined from our measurements agree rather well with bulk magnetic measurements. However, indexing all the reflections turned out to be rather difficult. There is no single propagation vector that would account for all the new reflections. After a trial-and-error approach we could index nearly all the reflections appearing at low temperature by using at least three propagation vectors. There are several possibilities. This is unfortunately an inevitable problem in powder diffraction. The first set of propagation vectors is $\mathbf{q_1}$ = (0 0 0), $\mathbf{q_2}$ = (0.2 0 0) and $\mathbf{q_3}$ = (0.4 0 0). We label this combination as Model I. This would

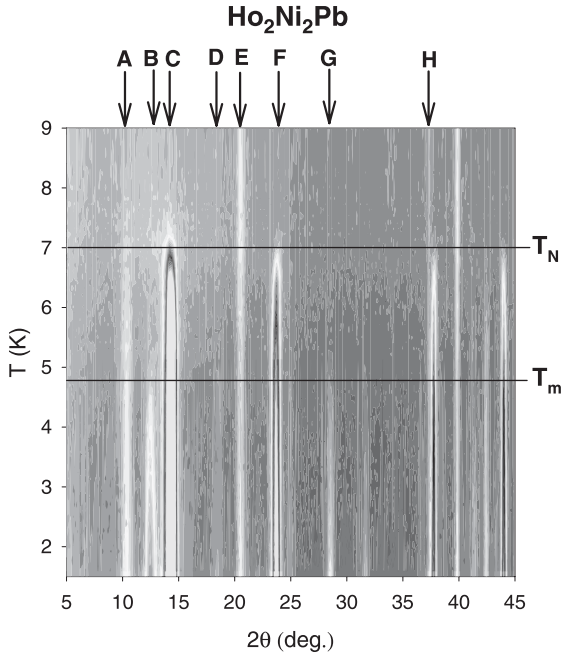

Fig. 3. Contour intensity plot showing the low angle portion of diffraction patterns taken on Ho_2Ni_2Pb versus temperature. The nine Bragg reflections denoted by arrows are discussed in the text.

suggest some kind of coupling of magnetic moments that repeats each crystallographic cell, in all three principal directions, together with an additional commensurate repetition that needs besides the principal propagation vector $\mathbf{q_2}$ = (0.2 0 0) also its second harmonics. Such combination occurs, for instance, in complicated helical structures. Another possibility is that besides the $\mathbf{q_1}$ = (0 0 0) and $\mathbf{q_2}$ = (0.2 0 0), one can use the third vector $\mathbf{q_3}$ = (0.6 0 0), which is the third harmonic of $\mathbf{q_2}$ (Model II). This situation appears in square modulated magnetic structures. Besides the two aforementioned possibilities that represent the simplest combinations one can use also more complex combinations like $\mathbf{q_1}$ = (0 0 0), $\mathbf{q_2}$ = (0.4 0 0) and $\mathbf{q_3}$ = (0.8 0 0) (Model III), $\mathbf{q_1}$ = (0 0 0), $\mathbf{q_2}$ = (0.4 0 0) and $\mathbf{q_3}$ = (1.2 0 0) (Model IV) or even $\mathbf{q_1}$ = (2.0 0 0), $\mathbf{q_2}$ = (0.4 0 0) and e.g. $\mathbf{q_3}$ = (1.2 0 0) (Model V) in which the first vector $\mathbf{q_1}$ = (2.0 0 0) is the fifth harmonic of the second one $\mathbf{q_2}$ = (0.4 0 0). All these combinations lead to complete indexing of reflections observed just below T_N. As the temperature further decreases, new set of reflections appear. Most of the reflections appear at positions indexable by the above mentioned propagation vectors. However, one of the reflections at the diffraction angle of about 2θ = 18.1 deg. (in Fig. 3 denoted by letter D) cannot be indexed within the given scheme. This calls either for another, a fourth, propagation vector, or the indexing scheme is wrong. Let us treat this problem later.

3.3 Temperature dependence of the magnetic signal: polycrystalline experiment

In Figures 4, 5 and 6 we show the temperature dependencies of integrated intensities of the eight reflections labeled in Figure 3 by capital letters A, ... H. They are divided into three groups – each shown in a separate figure. The intensity of the first group of reflections (see Fig. 4 represented by reflections A (indexable as (0 1 0)), C (indexable as (0.4 0 0)), and F (indexable as (0.6 1 0)) disappear around T_N = 7.0 K. The second group of reflections represented by B (indexable as (0.2 1 0)), D (non-indexable reflection) and G (indexable as (0.8 0 0)) vanish around 5 K (see Fig. 5, i.e. around the temperature of T_m = 4.8 K suggested in literature as being a transition between an AF structure and a structure with a ferromagnetic (F) component existing at lower temperatures [7]. Reflections E, and H (see Fig. 6) which were identified in Figure 2 as having indices (020) and (110), respectively, do not seemingly contain any magnetic contribution. A ferromagnetic component leads normally to a higher intensity below the relevant ordering temperature as compared to the paramagnetic phase. While the (020) reflection is truly temperature independent, the (110) reflection increases slightly with increasing temperature normally indicative either of the presence of extinction in the sample or of a slight movement of atomic positions. In our case, however, we attribute this observation to the proximity of stronger reflection that appears below T_N and difficulty to extract the intensity of (110) reflection exactly. In any case, we can exclude that the ground state of Ho_2Ni_2Pb is ferromagnetic as suggested by Gulay et al. [3] as this would lead to increase of at least one of the observed nuclear reflections. At the bottom of Figure 6 we show the temperature dependence of the background intensity in the vicinity of the A reflection, which increases with increasing temperature and saturates above T_N = 7.0 K. This observation is consistent with the expected incoherent contribution of the disordered magnetic moments that do not change above T_N and vanishes at low temperatures.

3.4 Possible ground-state magnetic structures

As can be easily seen from Figures 3 and 4, the strongest magnetic reflection at all temperatures is the reflection C. This reflection can be identified as being (0.4 0 0). Within the model I (reflection would have the index $(000)^{+-q_3}$) this would suggest this reflection to be the second harmonics of the (0.2 0 0) reflection (indexable as $(000)^{+-q_2}$)). However, no (0.2 0 0) reflection, which would be probably stronger than (0.4 0 0) and which would be at angle of 2θ = 7 deg. is visible in Figure 3. Thus, if we accept that the first harmonics should be the strongest we can disregard model I. For similar reasons we can rule out also models II and V. However, it has to be stressed that such conclusions are made with the assumption that the two propagation vectors belong to a single phase and represent two Fourier components of the same magnetic structure.

Let us for a moment consider the C reflection as being the fundamental one described by the propagation vector $\mathbf{q_2}$ = (0.4 0 0). This would imply the appearance of a sine-wave magnetic modulated structure in Ho_2Ni_2Pb just below the ordering temperature of 7.0 K. Since we deal with orthorhombic symmetry the sine wave can be

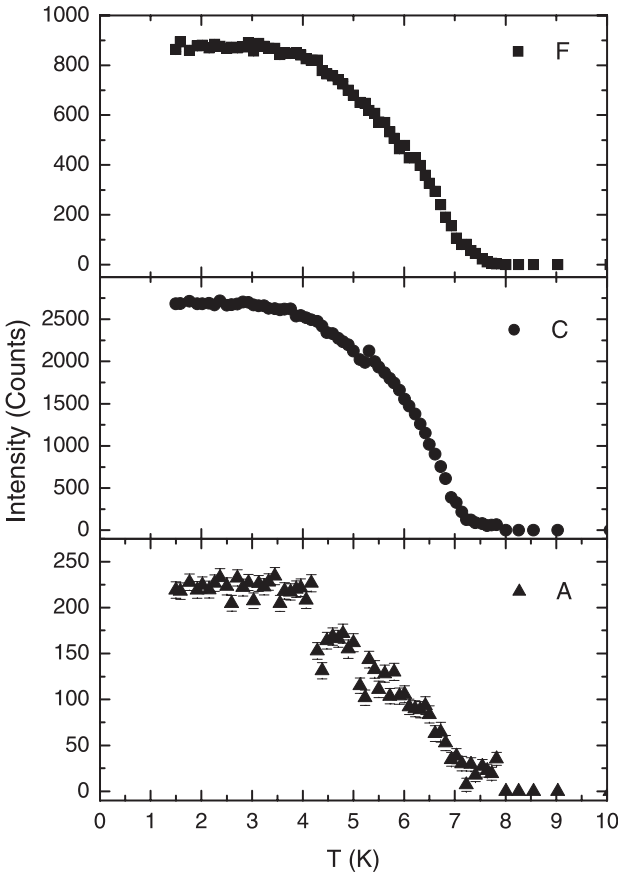

Fig. 4. The temperature dependence of the three reflections disappearing around $T_N = 7.0$ K that are denoted in Figure 3 by letters A, C and F.

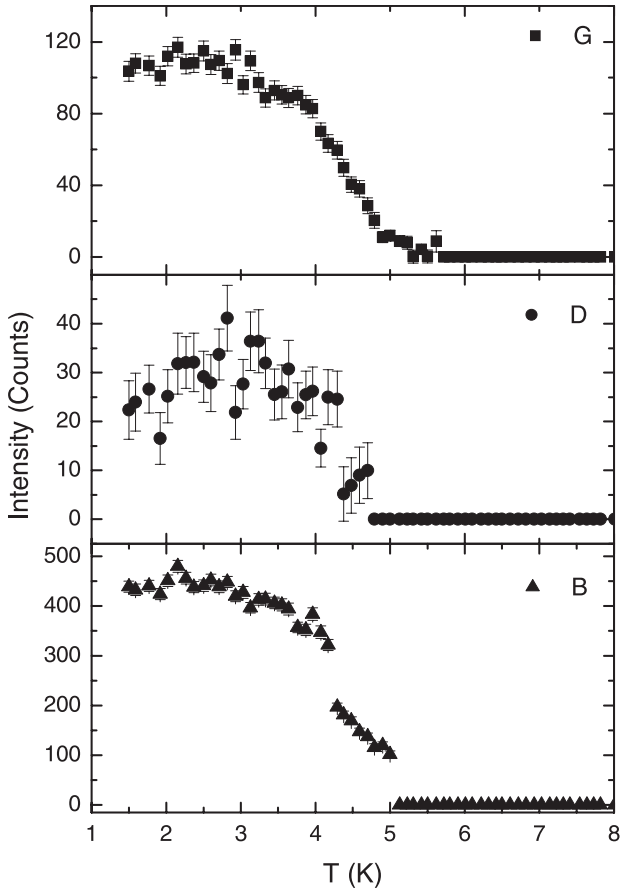

Fig. 5. The temperature dependence of the three reflections disappearing around $T_m = 4.8$ K that are denoted in Figure 3 by letters B, D and G.

either longitudinal or transversal [15]. While at temperatures in the vicinity of the $T_N = 7.0$ K one can expect truly sine-wave modulation, such a structure is unstable at lowest temperature, in the ground state. Normally, an equal-size magnetic moment arrangement is more stable. This can happen, e.g. for sine-wave modulated structure that square-up. In helical structures the moments might remain unequal. Thus, if the sine-wave magnetic structure appears just below $T_N = 7.0$ K a third-order component should appear at lower temperature. It is therefore natural to interpret the second set of magnetic reflections appearing around $T_m = 4.8$ K as the onset of the squaring-up. As can be seen from Figure 4, reflection C shows in this temperature range irregularity. Accordingly, model IV seems to be the most probable one.

With the help of group theory, that proposses, with the knowledge of the underlying paramagnetic crystal structure, propagation vectors, and the fact that the magnetic phase transition is of the second order (no distortion), one can generate all the allowed magnetic structures [16]. For the space group $Cmmm$ one finds that the four equivalent positions (the Ho atoms occupy the equivalent crystallographic positions 4(j)) are divided into two sub-sets (one having $x = 0$ and the other $x = 0.5$). This is caused by a translation $t(1/2, 1/2, 0)$ of the lattice that is not present in the so-called little group and which determines the possible coupling rules between moments [15]. Nevertheless, it is easy to see that these rules are identical within the two sub-sets. In the case of $\mathbf{q_1} = (0\ 0\ 0)$ one obtains either AF or F coupling between the moments that are directed along one of the principal axes. For $\mathbf{q_2} = (0.4\ 0\ 0)$ and $\mathbf{q_3} = (0.8\ 0\ 0)$ the situation is more complicated. Besides sine-wave modulated magnetic structures with moments pointing along principal axes, also more complicated magnetic structures with moments confined to the $a-b$ plane are possible. We have tried all the allowed combinations for models III and IV fixing the structural parameters except the lattice constants and atomic positional parameters equal to those found in the paramagnetic state.

It has to be noted that in the neutron experiment it is not possible for fundamental reasons to determine the value of the phases between the individual Fourier components and therefore without knowledge of other experimental facts (e.g. saturation magnetization per Ho ion) the true magnetic structure remains undetermined. To avoid this difficulty, we have used instead of three Fourier components an approach that introduces a larger magnetic unit cell along the a axis with respect to the chemical unit cell. The propagation vector $\mathbf{q_2} = (0.4\ 0\ 0)$ would suggest a 2.5 times larger magnetic unit cell. However, it is

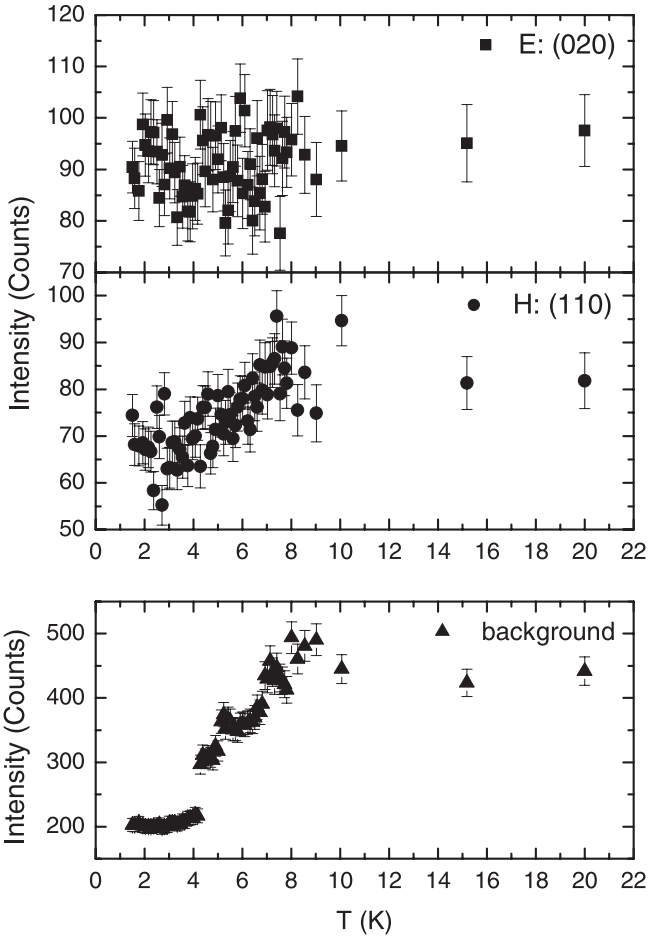

Fig. 6. The temperature dependence of the two reflections denoted in Figure 3 by letters E and H. Their indexes are (020) and (110) respectively. At the bottom the temperature dependence of the background in the vicinity of the A reflection is shown.

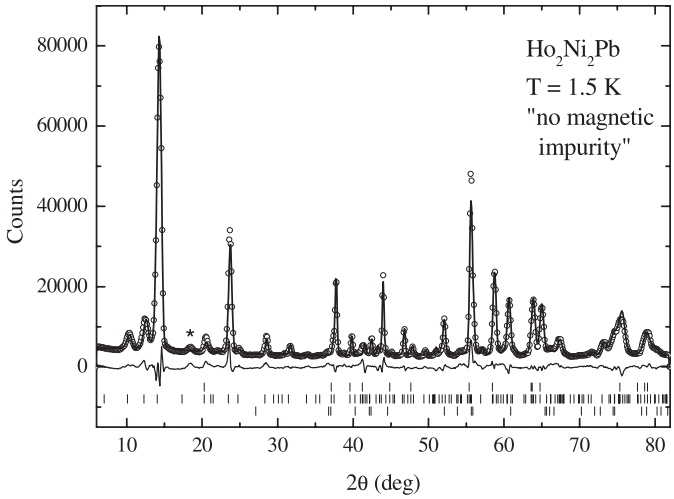

Fig. 7. The diffraction data (circles) of Ho_2Ni_2Pb taken at the lowest temperature of 1.5 K together with the best fit (the full line through points) supposing that only one magnetic phase exists in the sample and the difference between them (line at the bottom). Bragg reflection positions belonging to the crystal structure of HoNiPb, possible magnetic structure of the main Ho_2Ni_2Pb phase, and the crystal structure of Ho_2Ni_2Pb are tick-marked from the bottom upwards. By a star we denote the reflection at $2\theta = 18.1$ deg. that is not indexable.

more comfortable to introduce a magnetic cell that equals $5a \times 1b \times 1c$. In this way one can constrain the mutual coupling and the size of moments.

It became quite clear that in order to account for the observed (010) reflection (reflection A in Fig. 3) at the diffraction angle of about $2\theta = 10.0$ deg. one has to introduce a small but non-negligible AF coupling between the two chains of Ho moments (one chain consisting of Ho_1 and Ho_4, the other of Ho_2 and Ho_3). The moments in each chain being aligned ferromagnetically (the $\mathbf{q_1}$ = (0 0 0) component repeats every chemical unit cell). Orientation of the moments along the b axis does not lead to any intensity in the (010) reflection. This is possible only with orientation along the a or the c axis. A better agreement with the observed data has been found if the AF component lies along the c axis. This, however, leads to non-equivalence of the two Ho chains. The orientation of the moments along the a axis does not cause any such non-equivalence because in this case the $\mathbf{q_1}$ component is perpendicular to the other two Fourier components. There is, however, a strong argument against such a structure: a mixing of two irreducible representations would need to occur. Although not completely impossible, there are very few examples of such a mixing in the literature. We show the best fit to a five-times larger unit magnetic cell resulting from extensive fitting attempts in Figure 7. As can be seen, the quality of the fit (in this case to model IV) is not perfect but acceptable. In Figure 8 we show the possible magnetic structure of Ho_2Ni_2Pb resulting from this fit (assuming that all the propagation vectors belong to this phase). This structure is collinear, however not physical. As a manifestation of this (the non-equivalence) one can calculate the total magnetic moment in each of the two chains shown in Figure 8. For one of the chains (Ho_2-Ho_3) it is zero but for the other a net moment exists. This is not physical. The second problem is that the Ho moments are not of equal size within each of the chains. While this can happen if magnetic moments occupy inequivalent positions or if competing magnetic interactions exist in the system, it is rather improbable for a system with only one magnetic site in which a sine-wave magnetic structure develops just below the ordering temperature [15].

We have also tried to fit a magnetic structure to model III (with $\mathbf{q_1}$ = (0 0 0), $\mathbf{q_2}$ = (0.4 0 0) and $\mathbf{q_3}$ = (0.8 0 0)) supposing that it is non-collinear. The best fit consists of two cycloids, one having periodicity of $2.5a$ and the other of $1.25a$. Moreover, the two chains are "stretched" from each other leading to a complicated non-collinear arrangement of Ho moments. In terms of agreement factors it is only marginally worse with respect to the structure shown in Figure 8. Let us note that a similar magnetic structure to model III has been found for the isostructural compound Dy_2Ni_2Pb [9] in which two

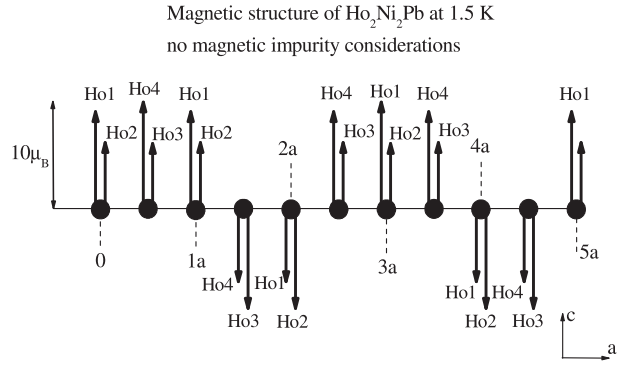

Fig. 8. Schematic representation of the magnetic structure of Ho_2Ni_2Pb at 1.5 K projected onto the $a-c$ plane and refined with the assumption of existence of only one magnetic phase in our sample (top). For a sake of clarity the Ho_1 and Ho_4 atoms are shifted to the left, Ho_2 and Ho_3 atoms to the right. Ho_1 and Ho_2 otherwise project onto the same place. Note that the two chains do not have the same total magnetic moment.

propagation vectors $\mathbf{q_1} = (0\ 0\ 0)$ and $\mathbf{q_2} = (0.333\ 0\ 0)$ exist. Theory, however, predicts that helical and related structures cannot exist in orthorhombic symmetries [15] unless there is an accidental degeneracy between two order parameters (mixing of irreducible representations). As a consequence, the magnetic phase transition has to be of the first order or two phase transitions must occur (as suggested in the literature for Ho_2Ni_2Pb [7]). Moreover, an easy-plane has to be present, and one has to neglect the effect of single-ion anisotropy. On the other hand, the advantage of such a complicated structure is that there is no reason to suppose equal-size magnetic moments. The non-collinear arrangement of unequal moments might be stable to the lowest temperatures. Thus, either we have to accept the fact that the two Ho chains are unequal, or our indexation of magnetic reflections is not completely correct.

3.5 Single crystal experiment

In Figure 9 we show two scans through the reciprocal lattice of the Ho_2Ni_2Pb taken at the lowest temperature of 1.5 K and in the paramagnetic state ($T = 20$ K) keeping the $k = 1$ (top) and $k = 0$ (bottom) index constant. The last index (l) is constrained to be zero due to geometry of the experiment. It is clear that at low temperatures several additional magnetic reflections are present that are missing in the paramagnetic state. Clearly, all the present peaks can be indexed with two of the three propagation vectors mentioned in Section 3.2. We have performed also scans through several other positions. Although not shown here we did not observe any additional intensity at the scattering angle $2\theta = 10$ deg., i.e. at the position that was identified as the reflection A and in polycrystalline experiment indexed (010).

In Figure 10 the temperature dependence of the normalized intensity measured at the peak of three representative reflections from Figure 9 is shown. Clearly, the

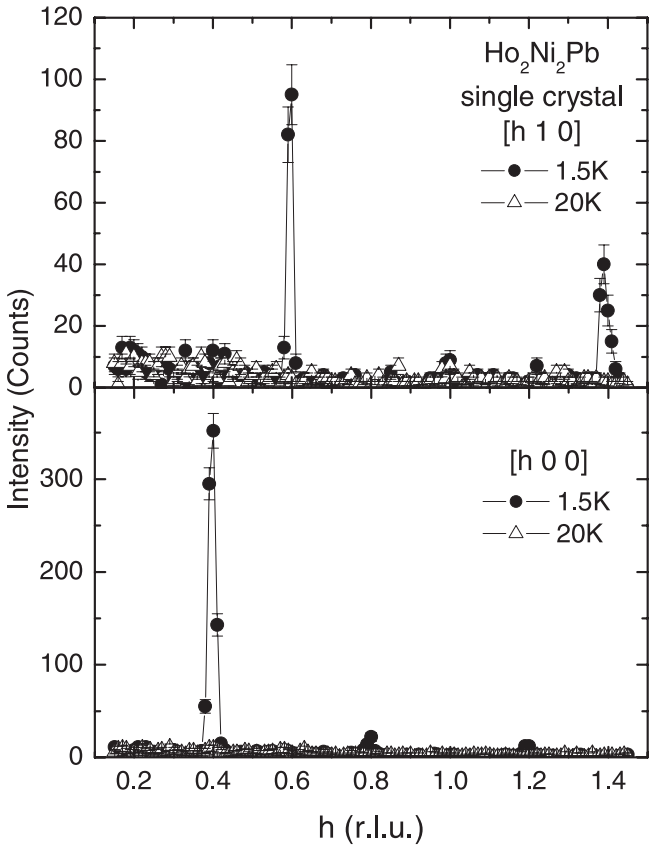

Fig. 9. Single crystal scans through the reciprocal lattice of the Ho_2Ni_2Pb at the lowest temperature of 1.5 K and at the paramagnetic state ($T = 20$ K) keeping the $k = 1$ (top) and $k = 0$ (bottom) constant. The last index is constrained to be zero due to geometry of the experiment.

magnetic phase transition $T_N = 7.0$ K can be associated with the appearance of the (0.4 0 0) reflection. The other magnetic phase transition at $T_m = 4.8$ K can be associated with a sizable appearance of the (0.8 0 0) reflection. However, this reflection exists already above this temperature - it appears just below the $T_N = 7.0$ K. Another important result of the single-crystal experiment is the appearance of the (1.2 0 0) reflection at temperatures lower than $T_s = 3.0$ K. We consider this temperature as the onset of the squaring-up of the magnetic structure. Thus, we can now exclude from our considerations also model IV. Furthermore, the non-existence of the (010) reflection eliminates the presence of the propagation vector $\mathbf{q_1} = (0\ 0\ 0)$. As we could not find any other propagation vector having the third index zero it suggests either that the reflections A ($2\theta = 10.0$ deg.) and D ($2\theta = 18.1$ deg.) are indexable with propagation vector having the third component non-zero or that these two reflections originate from an impurity.

3.6 Ground-state magnetic structure: impurity effect

In Section 3.2 we have mentioned that at the lowest temperature there is one magnetic reflection at the scattering

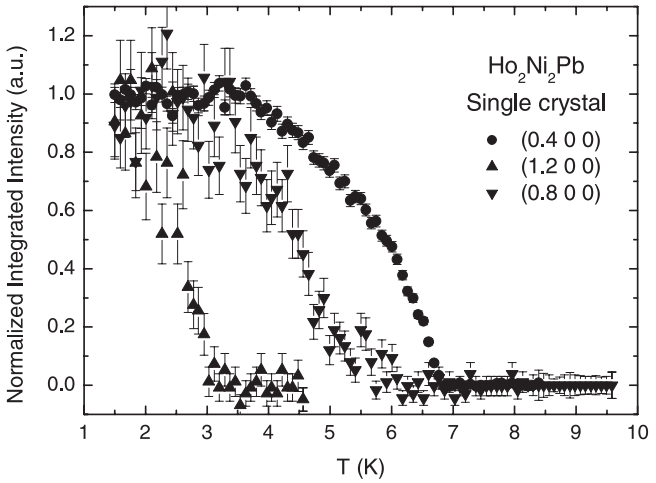

Fig. 10. The temperature dependence of the intensity at three reciprocal positions measured on a tiny single crystal of Ho_2Ni_2Pb and normalized to their intensities at 1.5 K. The real intensities at 1.5 K are approximately 1460 counts for the (0.4 0 0), 100 counts for the (0.4 0 0) and 50 counts for the (1.2 0 0) reflection respectively.

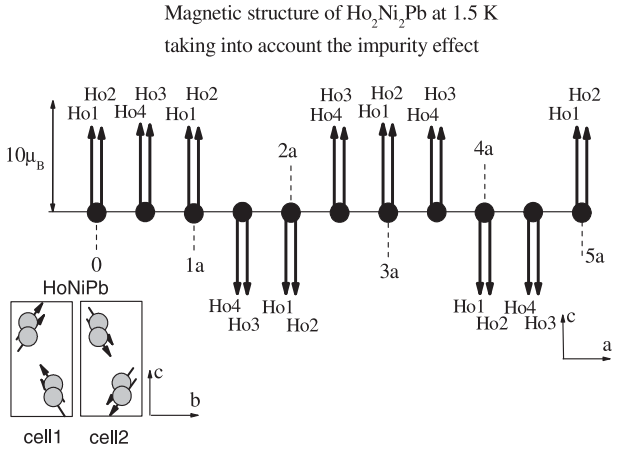

Fig. 11. Schematic representation of the magnetic structure of Ho_2Ni_2Pb at 1.5 K projected onto the $a-c$ plane and refined with the assumption of the existence of a minority HoNiPb magnetic phase in our sample that has doubling of the magnetic structure along the a axis. For the sake of clarity the Ho_1 and Ho_4 atoms are shifted to the left, Ho_2 and Ho_3 atoms to the right. Ho_1 and Ho_2 otherwise project onto the same place. Note that all the moments carry nearly the same magnetic moment.

angle of $2\theta = 18.1$ deg. that is not indexable with any of the three propagation vectors mentioned above. Moreover, in Section 3.5 we showed that the identification of the magnetic reflection at the scattering angle $2\theta = 10.0$ deg., belonging to the main phase and being (010), leads to an inequivalency of the two Ho magnetic moment chains. Let us now consider these two reflections in more details. The explanation of the former reflection is possible only with the help of a fourth propagation vector or by vaguely stating that it originates from some magnetic impurity. To explain the latter reflection one can claim that a distortion of the crystal structure appears at the magnetic phase transition $T_N = 7.0$ K. The transition would be then of the first-order type and all the conclusions obtained from the group analysis would be invalid. As a consequence, helical or cycloidal magnetic structures would be allowed. Another consequence of the distortion might be a loss of the symmetry element responsible for extinction of the (010) reflection in the paramagnetic state. A similar observation was made in the case of the isostructural Dy_2Ni_2Pb [9]. In order to gain information regarding the possible structural distortion we have performed recently powder X-ray diffraction on Dy_2Ni_2Pb at low temperatures [17]. No sign of any distortion has been found below $T_N = 14.5$ K of this system. It is most likely that Ho_2Ni_2Pb and Dy_2Ni_2Pb are very similar in this respect. We can therefore rule out that a distortion is responsible for appearance of the low-temperature reflection at $2\theta = 10.0$ deg. Furthermore, this would be observable also in the single crystal experiment (Sect. 3.5). This, in turn, suggests that this reflection is of magnetic origin. After extensive attempts to index both reflections we have found out that both are accounted for if one assumes that the minority HoNiPb phase orders magnetically with a doubling of its crystallographic unit cell along the a axis. Then, the reflection at $2\theta = 10.0$ deg. can be indexed as (100) and the other one at $2\theta = 18.1$ deg. as (001) within the doubled magnetic unit cell. Let us note that we can now index also the very small reflection at $2\theta = 38.5$ deg. – it has indices (111).

With this knowledge we have tried to fit the 1.5 K pattern considering four different phases. Besides the crystal structures of Ho_2Ni_2Pb and HoNiPb and the magnetic structure of Ho_2Ni_2Pb we tried to model also the magnetic structure of HoNiPb. The group analysis supposing the propagation vector $\mathbf{q_{HoNiPb}} = (0.5\ 0\ 0)$ leads to conclusion that Ho magnetic moments in HoNiPb can be coupled either in an AF or a F manner and oriented along the principal axes. Although it is hard to distinguish which of the possible models fit the intensities better, we have arrived at a relatively good description of these reflections by keeping the Ho moment to be 10 μ_B and the scaling factor acquired from the paramagnetic fit. The proposed magnetic structure for HoNiPb is shown in the inset of the Figure 11.

The fact that some of the Bragg reflections at low temperatures are due to magnetic order of the minority phase has a significant consequence on the magnetic structure of the main Ho_2Ni_2Pb phase. Namely, there is no need for any difference between the two magnetic chains running along the a axis. In Figure 12 we now show the best fit to the diffraction pattern recorded at 1.5 K using the $5a\times b\times c$ magnetic unit cell. For numerical results see Table 2. The resulting magnetic structure proposed for Ho_2Ni_2Pb at low temperatures is shown in Figure 11. As can be seen from Figure 11 , the moments are oriented along the c axis and are equal in size. The magnitude of the Ho moment attains the value of about 8.2 μ_B at 1.5 K. This is 18% less than the value 10 μ_B expected for a free Ho^3+ ion. On the other hand, this structure consists of equal-size moments and is symmetrical. There is a net (uncompensated)

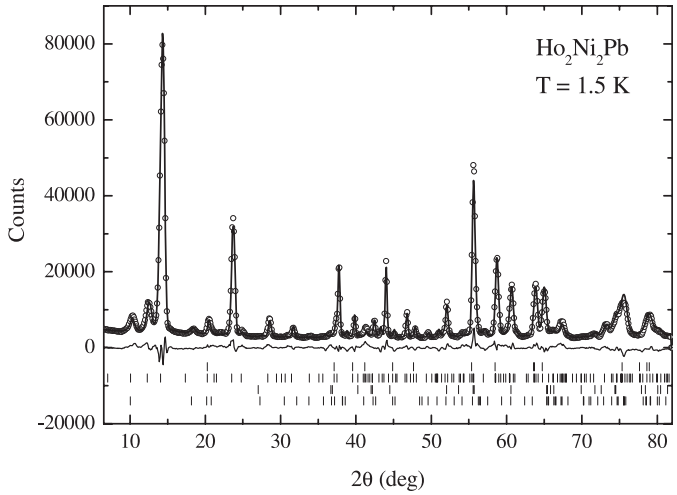

Fig. 12. The diffraction data (circles) of Ho_2Ni_2Pb taken at the lowest temperature of 1.5 K together with the best fit (the full line through points) and the difference between them (line at the bottom). Bragg reflection positions belonging to the magnetic structure of HoNiPb, crystal structure of HoNiPb, magnetic structure of the main Ho_2Ni_2Pb phase and the crystal structure of Ho_2Ni_2Pb are tick-marked from the bottom upwards. For numerical results see Table 2.

magnetic moment of $4 \times 8.2 = 32.8\ \mu_B$ per magnetic unit cell corresponding to $1.6\ \mu_B$ per Ho ion. Both the magnetic moment value per Ho ion and the zero-field uncompensated magnetic moment agree rather well with the magnetization experiment [4] that shows saturated magnetization of $8.3\ \mu_B$/Ho and low-field magnetization of about $1.7\ \mu_B$/Ho. There is, however, one significant difference between the neutron result and magnetic bulk measurements. A magnetization experiment on a small single crystal that originates from the same batch revealed that the easy magnetization direction is parallel to the a axis in contrast to the neutron results that suggest Ho magnetic moments being directed along the c axis.

In order to gain additional information regarding the easy magnetization direction from neutron experiment we have applied a field of 4.5 T at low temperatures to the powder sample. The sample was a loose powder with grain size small enough to suppose that each grain was monocrystalline and able to change its orientation via a rotation. First we have recorded the powder pattern in zero field, then, keeping it at low T, we have applied a field of 4.5 T and vibrated the sample tube whilst rotating it in the magnetic field. In this way we have achieved presumably almost complete alignment of the easy magnetization axis of the crystallites along the applied field. As is clear from Figure 13, the easy axis is parallel or very close to the c axis because except for the (111) reflection all the reflections in the 4.5 T pattern have the third index equal to zero. Thus, we can conclude that the identification of axes in the magnetization experiment is not correct.

Table 2. Refined magnetic parameters of Ho_2Ni_2Pb determined at 1.5 K and at 5.0 K.

$T = 1.5$ K		
Atom	Pos. parameters	Mag.moment
Ho1	0 0.3652(4) 0.5	8.1(1)
Ho2	0 0.6348(4) 0.5	8.1(1)
Ho3	0.5 0.8652(4) 0.5	8.3(1)
Ho4	0.5 0.1348(4) 0.5	8.3(1)
Ni	0 0.1999(7) 0	0.0(fixed)
Pb	0 0 0	0.0(fixed)
net moment		1.6 (2)
Lattice constants:		
$a = 400.21(7)$ pm	$b = 1390.3(3)$ pm	$c = 361.25(7)$ pm
Agreement factors:		
$\chi^2 = 12.26$	$R_p = 6.77\%$	$R_M = 7.72\%$
$T = 5.0$ K		
Atom	Pos. parameters	Mag.moment
Ho1	0 0.3652(4) 0.5	5.4(2)
Ho2	0 0.6348(4) 0.5	5.4(2)
Ho3	0.5 0.8652(4) 0.5	8.1(2)
Ho4	0.5 0.1348(4) 0.5	8.1(2)
Ni	0 0.1999(7) 0	0.0(fixed)
Pb	0 0 0	0.0(fixed)
net moment		1.0 (2)
Lattice constants:		
$a = 400.24(7)$ pm	$b = 1390.2(3)$ pm	$c = 361.22(8)$ pm
Agreement factors:		
$\chi^2 = 11.2$	$R_p = 5.73\%$	$R_M = 6.70\%$

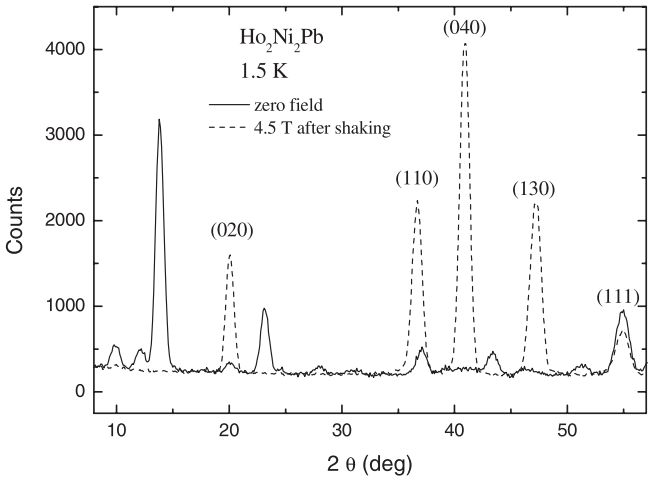

Fig. 13. The diffraction data of Ho_2Ni_2Pb taken at the lowest temperature of 1.5 K in zero field (the full line) and at the field of 4.5 T after shaking the sample tube to achieve alignment of the grains with their easy magnetization direction along the applied field (broken line). Note that except for the (111) reflection all the Bragg reflections in field have the last index equal to zero. This suggests that the easy magnetization direction in Ho_2Ni_2Pb is parallel to the c axis.

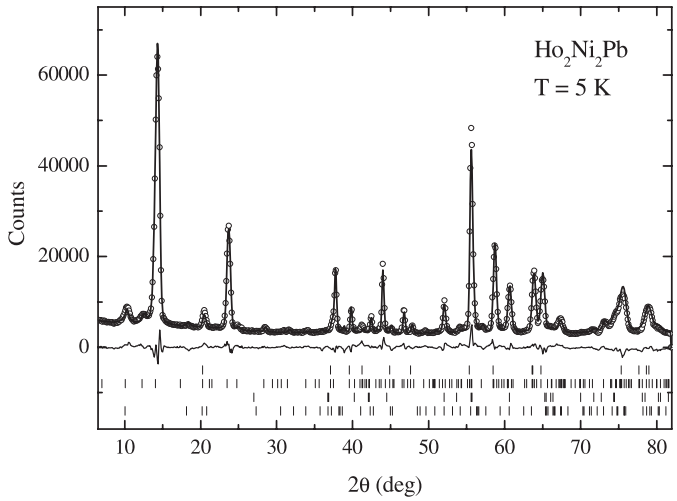

Fig. 14. The diffraction data (circles) of Ho_2Ni_2Pb taken at 5 K together with the best fit (the solid line through points) and the difference between them (line at the bottom). Bragg reflection positions belonging to the magnetic structure of HoNiPb, crystal structure of HoNiPb, magnetic structure of the main Ho_2Ni_2Pb phase and the crystal structure of Ho_2Ni_2Pb are tick-marked from the bottom upwards. For numerical results see Table 2.

3.7 Magnetic structure at elevated temperatures

In Section 3.3 we have shown the temperature dependence of the integrated intensity of eight reflections obtained from the powder experiment and in Section 3.5 of three reflections measured on a single crystal. With the knowledge of the effect of the impurity effect we are able now to resolve the changes in the magnetic structure of Ho_2Ni_2Pb caused by an increase of temperature and the temperature dependence of individual Ho magnetic moments. In Figure 14 we show the best fit to the diffraction pattern recorded at 5 K using the $5a \times b \times c$ magnetic unit cell. To obtain this fit we have kept all the structural parameters except for the lattice constants and position of Ho ions equal to those obtained at low temperatures. We have also assumed that the magnetic structure of the impurity phase remains the same, so that for HoNiPb we left only the moment magnitude as a free parameter. As can be seen, all the stronger magnetic reflections of Ho_2Ni_2Pb that were present at 1.5 K are also discernible in this pattern, i.e. above $T_m = 4.8$ K. The corresponding magnetic structure is shown in Figure 15. It can be characterized as a simple collinear transversal sine-wave modulated commensurate magnetic structure. The amplitude of the sine wave amounts to 8.1 μ_B. So, the fundamental difference with respect to the magnetic structure at low temperatures is that here, at 5 K, Ho moments are modulated and no sizable net magnetic moment exists. However, it is still not equal to zero, thereby explaining a remaining small intensity of the reflection at $2\theta = 12.0$ deg. Numerical results are given in Table 2.

The temperature dependence of the two Ho moments (denoted in Fig. 15 as Ho_1 and Ho_4 in the first chemical unit cell and Ho_4 from the second unit cell) is shown in

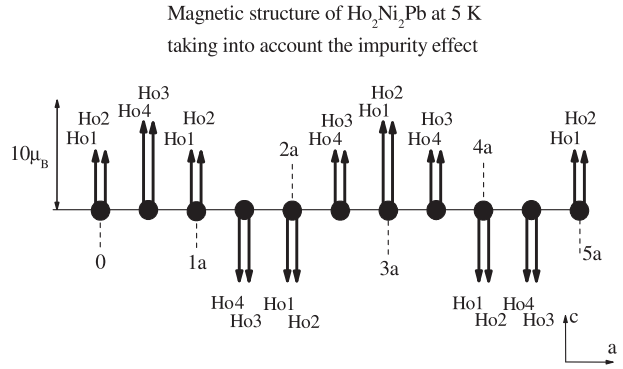

Fig. 15. Schematic representation of the magnetic structure of Ho_2Ni_2Pb at 5 K projected onto the $a-c$ plane and refined with the assumption of the existence of a magnetic impurity HoNiPb phase in our sample.

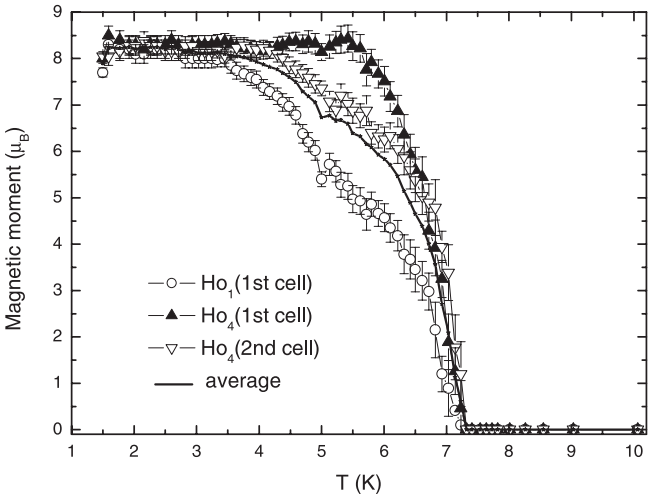

Fig. 16. The temperature dependence of three individual magnetic moments, namely Ho_1 and Ho_4 in the first chemical unit cell and Ho_4 from the second cell, all disappearing around $T_N = 7.0$ K. The full line shows the average moment.

Figure 16. These values have been obtained by fitting the the diffraction pattern to the same type of magnetic structure as in the case of the 1.5 and the 5 K patterns: using the $5a \times b \times c$ magnetic unit cell. In these fits we have kept all the structural parameters except for the lattice constants equal to those obtained at low temperatures. The only additional free parameters were the background parameters and constrained magnetic moment values. In Figure 16 also the average magnetic moment obtained by a summation of moment magnitudes within the magnetic unit cell divided by the number of ions in the cell is shown. As can be seen, while the magnitude of Ho_4 in the first chemical cell remains nearly constant with increasing the temperature up to about 5.5 K, Ho_1 moment starts to decrease around 3.5 K, i.e. around the same temperature where also the (1.2 0 0) reflection disappears (see Fig. 10) and which we consider as the temperature T_s below which a squaring up of the magnetic structure occurs. Let us note that especially the single crystal experiment shed important light on this issue as it revealed

the existence of a temperature T_s below which the third order harmonic appears. Although the Ho_1 moment disappears only in the vicinity of T_N it shows an inflection point around $T_m = 4.8$ K, a temperature suggested in the literature as an antiferromagnetic-ferromagnetic phase transition. It seems natural to interpret the $T_m = 4.8$ K as the temperature below which the magnetic structure of Ho_2Ni_2Pb can be considered as an uncompensated antiferromagnetic structure leading to a non-zero net magnetic moment although the full squaring-up appears only below $T_s = 3.0$ K. We do not see, however, any irregularity in the temperature dependence of the net magnetization of the sample as the function of temperature in this temperature range. Also the temperature dependence of the magnetic moment magnitude of the HoNiPb secondary phase does not show any irregularities around 5 K. The Ho_4 in the second chemical cell remains nearly constant up to about 3.5 K and then starts to decrease in a similar way as the average moment. The small discrepancy between fitted results obtained from extensive data taken at 1.5 and 5 K and from the short scans as a function of temperature, results from lower statistics and number of refined parameters in the case of the short scans. Finally, it seems that all the moments disappear at slightly higher temperatures compared to values mentioned in the literature.

4 Discussion

Refinement of the paramagnetic diffractogram showed clearly that besides the main Ho_2Ni_2Pb phase having the *Cmmm* space group another phase that was identified as HoNiPb can be discerned. Nevertheless, due to small intensity of relevant peaks it was rather difficult to obtain reliable crystal structure parameters for the secondary phase. Furthermore, the situation is complicated due to problems with preferential orientation of crystallites. The crystal structure of Ho_2Ni_2Pb has very different lattice constants. We had to introduce the preferential orientation already at the stage of refining the paramagnetic 20 K pattern.

The literature suggests two magnetic phase transitions to be present in Ho_2Ni_2Pb. The first one, at $T_N = 7.0$ K, was suggested to be from the paramagnetic state to an antiferromagnetic state [4,7,8]. However, Gulay et al. [3] report for Ho_2Ni_2Pb that a ferromagnetic phase transition takes place at $T_C = 7.0$ K. Neutron data clearly support the first hypothesis, albeit that the transition has been found at slightly higher temperature. This could be due to a temperature gradient in the cryostat. A short-range magnetic order in Ho_2Ni_2Pb spanning T_N can be also a factor in determining the phase transition temperature.

In the neutron data analysis we have supposed that all the symmetry operations of the crystal lattice are preserved below T_N. Then, symmetry group analysis yields possible magnetic structures. This approach can be used only if the magnetic phase transition is of the second order and no distortion takes place. The absence of any sign of crystal structure distortion in our sample and in the related Dy_2Ni_2Pb that was checked by X-ray diffraction at low temperatures gives us confidence that such an approach is justified. We note that all the low-angle reflections are resolution limited. At first we have assumed that all the magnetic Bragg reflections appearing below T_N belong to the main phase. The resulting ground state magnetic structure at 1.5 K that gives among all the allowed models the best agreement with experimental data is rather unusual. Although it was found to be collinear with a moment magnitude of about 10 μ_B/Ho, it is unphysical because the two chains of moments become nonequivalent. More complicated magnetic structures that consider even a small crystal structure distortions provide neither a better description of observed data nor a resulting structure that is physically acceptable. Moreover, within the recognized scheme of three propagation vectors, it is impossible to account for one weak magnetic reflection appearing around $2\theta = 18.1$ deg. that requires the existence of another, fourth, propagation vector.

When we, however, suppose that one of the magnetic reflections, namely that at $2\theta = 10.0$ deg. originates from the magnetic order of the secondary phase the situation is drastically changed. Namely, the resulting magnetic structure (see Fig. 11) at the lowest temperature consists of Ho moments that are collinear and equal in size. This is actually expected from entropy arguments [15].

The refined magnetic structure has, however, one drawback. The moments are noticeably reduced with respect to the free Ho^{3+} ion value of 10 μ_B. This is a signature of crystal electric field (CEF) effects. We believe that the refined moment value of 8.3 μ_B is correct as it agrees very well with the saturated magnetization value [4]. Our neutron diffraction in magnetic fields revealed, however, that the easy magnetization direction is along the c axis and not parallel to the a axis as suggested by magnetization measurement on a single crystal.

The Ho atoms form two nearly triangular chains and we argue at this point that such an arrangement can lead to frustration effects due to competing AF and F interactions along the three links connecting Ho atoms. Competing interaction in the presence of magnetocrystalline anisotropy are a well-known origin for unequal or reduced moments and can lead to very complicated noncollinear magnetic structures [15] especially in rare-earth compounds [18].

As the temperature increases the squared magnetic structure evolves into an ordinary sine-wave modulated one, still with moments being locked along the c axis.

5 Conclusions

We have presented the results of comprehensive powder and single crystal neutron diffraction measurements in fields up to 4.5 T performed on Ho_2Ni_2Pb. The paramagnetic powder diffraction pattern could be explained only by supposing that about 5% of the HoNiPb secondary phase is present in the sample. Based upon fitting of neutron diffraction patterns to models allowed by symmetry,

assuming that also the HoNiPb orders antiferromagnetically, the Ho_2Ni_2Pb compound has been found to have a relatively simple collinear uncompensated antiferromagnetic structure (three moments up, two down along the c axis, magnitude 8.3 μ_B/Ho) that can be described either by two commensurate propagation vectors $\mathbf{q_2} = (0.4\ 0\ 0)$ and $\mathbf{q_3} = (0.8\ 0\ 0)$ or by using a magnetic unit cell that is, compared to the chemical lattice, five times larger along the a axis. Contribution described by the remaining propagation vector $\mathbf{q_1} = (0\ 0\ 0)$ was found to belong to HoNiPb. If ascribed to Ho_2Ni_2Pb it leads to an unphysical nonequivalence of chains. The reduced size of Ho moment is attributed to competing interactions and crystal-field effects. It agrees well with magnetization measurements.

Bulk measurements suggest two magnetic phase transitions in Ho_2Ni_2Pb. The $T_N = 7.0$ K is clearly identified by appearance of magnetic Bragg reflections indexable by a propagation vector $\mathbf{q_2} = (0.4\ 0\ 0)$. The corresponding magnetic structure is a simple transversal sine-wave propagating along the a axis. The second magnetic phase transition at $T_m = 4.8$ K was suggested to be of ferromagnetic nature. According to our neutron diffraction experiments T_m corresponds to the appearance of the $\mathbf{q_3} = (0.8\ 0\ 0)$ propagation vector that marks a change in the moment configuration from a simple sine wave to a more complex one. Finally, the single-crystal experiment revealed a complete squaring up of the Ho moment configuration below $T_s = 3.0$ K that is manifested by the appearance of the third harmonic.

This work was supported by the Dutch NWO and FOM Foundations, CONACyT (Mexico) through grants G-25851 and 39643-F and by the European Commission contract HPRI-CT-2001-00138 Access to Research Infrastructures. We wish to acknowledge the competent assistance of R.W.A Hendrikx and T.J. Gortenmulder in the sample preparation and analysis.

References

1. *Handbook of Magnetic Materials*, Vols. 1–13, edited by K.H.J. Buschow (Elsevier North Holland, Amsterdam, (1980-2001)
2. L.D. Gulay, Y.M. Kalychak, M. Wolcyrz, J. Alloys Compd. **311**, 228 (2000)
3. L.D. Gulay, K. Hiebl, J. Alloys Compd. **351**, 35 (2003)
4. A.D. Chinchure, E. Muñoz-Sandoval, J.A. Mydosh, Phys. Rev. B **66**, 020409(R) (2002)
5. J.L. Daams et al., *Atlas of Crystal Structure Types for Intermetallic Phases* (ASM International, 1991)
6. A.D. Chinchure, E. Muñoz-Sandoval, J.A. Mydosh, Phys. Rev. B **64**, 020404(R) (2001)
7. E. Muñoz-Sandoval, A.D. Chinchure, R.W.A. Hendrikx, J.A. Mydosh, Europhys. Lett. **56**, 302 (2001)
8. A.D. Chinchure, E. Muñoz-Sandoval, T.J. Gortenmulder, R.W.A. Hendrikx, J.A. Mydosh, J. Alloys Compd. **359**, 5 (2003)
9. K. Prokeš, E. Muñoz-Sandoval, A.D. Chinchure, J.A. Mydosh, Phys. Rev. B **68**, 134427 (2003)
10. H.M. Rietveld, J. Appl. Cryst. **2**, 65 (1969)
11. T. Roisnel, J. Rodriguez-Charvajal, WinPLOTR (May 2003) computer code, unpublished
12. V.F. Sears, Neutron News **3**, 26 (1992)
13. L.D. Gulay, K. Hiebl, J. Alloys Compd. **339**, 46 (2002)
14. E. Muñoz-Sandoval, A. Díaz-Ortiz, A.D. Chinchure, J.A. Mydosh, J. Alloys Compd. **369**, 260 (2004)
15. J. Rossat-Mignod, in *Neutron Physics*, Vol. 23C, edited by K. Skold, D.L. Price (Academic Press, 1987), p. 69
16. E.F. Bertaut, Acta Crystallogr. A **24**, 217 (1968)
17. S. Daniš, K. Prokeš, E. Muñoz-Sandoval, A.D. Chinchure, J.A. Mydosh (2003), unpublished
18. W. Suski, in *Handbook on the Physics and Chemistry of Rare Earths*, Vol. 22, Chap. 146, edited by K.A. Gschneidner Jr., L. Eyring (Elsevier Science, Amsterdam, 1996), p. 143